

## Lattice parameter of $\text{Si}_{1-x-y}\text{Ge}_x\text{C}_y$ alloys

D. De Salvador, M. Petrovich,\* M. Berti, F. Romanato,† E. Napolitani, and A. Drigo  
 INFN at the Physics Department, University of Padova, Via Marzolo 8, 35131 Padova, Italy

J. Stangl, S. Zerlauth, M. Mühlberger, F. Schäffler, and G. Bauer  
 Institut für Halbleiterphysik, Johannes Kepler Universität Linz, Altenbergerstrasse 69, A-4040 Linz, Austria

P. C. Kelires

Physics Department, University of Crete, P.O. Box 2208, 710 03 Heraclion, Crete, Greece  
 and Foundation for Research and Technology–Hellas (FORTH), P.O. Box 1527, 711 10 Heraclion, Crete, Greece  
 (Received 15 November 1999)

The introduction of carbon into silicon-germanium–based heterostructures offers increased flexibility in tailoring their strain state and electronic properties. Still, however, fundamental physical properties such as the lattice parameter and the elastic properties of  $\text{Si}_{1-x-y}\text{Ge}_x\text{C}_y$  random alloys are not precisely known. In this paper, we present a quantitative study of the effect of carbon on the lattice parameter of  $\text{Si}_{1-x-y}\text{Ge}_x\text{C}_y$  alloys in the technologically relevant range of Ge and C compositions. A strong deviation from Vegard's rule is experimentally and theoretically derived. The influence of the correlation between Ge and C on the lattice parameter is discussed. The results allow us to establish the compensation ratio  $\nu$  of Ge to C concentrations (where the  $\text{Si}_{1-x-y}\text{Ge}_x\text{C}_y$  epilayer is lattice matched to Si), for which we find a value of  $\nu=12$ .

### I. INTRODUCTION

The fundamental physical properties and possible device applications of  $\text{Si}/\text{Si}_{1-x}\text{Ge}_x$  heterostructures have been studied extensively in the past ten years. Recently, the introduction of carbon into the binary alloy opened some new ways toward the use of Si-based heterostructures, because it offers improved mechanical stability, manipulation of the lattice constant, and the possibility of tailoring the band discontinuities through composition and associated strain modulation. Even devices based on  $\text{Si}_{1-x-y}\text{Ge}_x\text{C}_y$  heterostructures such as a heterobipolar transistor with a  $\text{Si}_{1-x-y}\text{Ge}_x\text{C}_y$  base region have been suggested and realized (see Refs. 1,2 for a review). Yet, the fundamental physical properties of the  $\text{Si}_{1-x-y}\text{Ge}_x\text{C}_y$  alloy are not fully understood, and some issues are strongly debated.

From the electronic properties point of view, intense research focuses on how the band gap and band offsets are varied with carbon content.<sup>3–5</sup> As far as structural properties are concerned, an important issue that attracted attention is the extent to which incorporation of carbon into the  $\text{Si}_{1-x}\text{Ge}_x$  lattice compensates the built-in compressive strain due to the mismatch with the Si substrate. This is ultimately related with the lattice response to carbon incorporation. It was customary among researchers to extract the carbon content in the alloy using Vegard's law, which demands that the lattice parameters as well as the elastic constants adhere to a linear interpolation scheme of the elemental constants. This rule leads to a strain compensation ratio  $\nu$ , i.e., the ratio of Ge and C concentrations  $x$  and  $y$ , respectively, where the net strain of the  $\text{Si}_{1-x-y}\text{Ge}_x\text{C}_y$  compound becomes zero, equal to 8.7. However, theoretical Monte Carlo (MC) simulations of the incorporation processes and lattice relaxation by one of the authors<sup>6–8</sup> predicted strong negative deviations from Vegard's law in the ternary alloy, both for the lattice param-

eters and the elastic constants, leading to a strain compensation ratio of  $\nu=11.5$ . This implies that the use of Vegard's rule results in the overestimation of carbon content by  $\sim 30\%$ , which in its turn has significant consequences on the correct description of the band-gap variation with carbon content.<sup>9</sup> Similar behavior has also been reported by tight-binding–like quantum molecular dynamics calculations, utilizing localized orbitals,<sup>10</sup> which found an even larger ratio of  $\nu=15$ .

Deviations from the linear rules have been found to exist in related binary systems as well. In 1964, Dismukes *et al.* reported a slight deviation from Vegard's rule in the  $\text{Si}_{1-x}\text{Ge}_x$  system,<sup>11</sup> verified by theoretical calculations.<sup>12,13</sup> Larger deviations have been predicted by theoretical MC simulations<sup>14</sup> to exist in the carbon containing  $\text{Si}_{1-x}\text{C}_x$  alloy, having a large atomic size mismatch between the constituent species, that was verified by a comparison of x-ray diffraction and ion backscattering techniques.<sup>15</sup> Therefore, it is not surprising that such deviations exist in the ternary alloy. The interest in this case, which is more complicated due to the presence of Ge, is to unravel any influence that the Ge–C correlations in the Si lattice might have on the lattice parameters, and to measure the compensation ratio precisely.

An earlier experimental study by Meléndez-Lira *et al.*<sup>16</sup> indicated that the compensation ratio might be around 14. Another work by Segó *et al.*<sup>17</sup> found a ratio of only 5 (undercompensation). This was attributed by Windl *et al.*,<sup>10</sup> who calculated the influence of different possible C interstitial configurations on strain, to the high percentage of interstitial carbon ( $\sim 50\%$ ) in the samples reported in Ref. 17. While it is plausible that the effect of interstitial carbon is to lower the value of  $\nu$ , such a low value is rather unexpected. Therefore, further research is needed to establish the effect of interstitial carbon on  $\nu$ . Several experimental studies<sup>18–20</sup> indicate that the substitutional fraction, i.e., the fraction of C atoms incor-

porated substitutionally, depends on growth conditions, such as substrate temperature and adatom fluxes in molecular beam epitaxy (MBE) techniques.

In this paper, we report on a combined experimental and theoretical effort to shed more light on these issues. Our main objectives are (a) to determine the compensation ratio; (b) to study the influence of Ge–C correlations on the variation of lattice parameters; and (c) to study the influence of interstitial carbon on the lattice constants. For all three targets, a number of complementary experimental techniques have been utilized. The chemical composition of several MBE-grown  $\text{Si}_{1-x-y}\text{Ge}_x\text{C}_y$  epilayer series was determined by ion backscattering experiments, namely Rutherford backscattering (RBS) and resonant backscattering (rBS), that were also used to determine the substitutional fractions. The combination of these data with the lattice parameter of the epilayers determined by x-ray diffraction (XRD) yielded the bulk lattice parameter of  $\text{Si}_{1-x-y}\text{Ge}_x\text{C}_y$ . For the calculation of the alloy lattice parameter and especially for fulfilling objective (b), extensive MC simulations have been carried out.

The paper is organized as follows: In Sec. II the experimental methods used for the investigations are presented, Sec. III describes the theoretical methods. In Sec. IV the experimental results are presented, and finally Sec. V discusses the results as well as the correspondence of experiment and theory.

## II. EXPERIMENTAL METHODS

### A. Sample growth

Three series of samples characterized by different Ge compositions have been fabricated by MBE using  $e^-$ -beam evaporators for Si, Ge, and C. The overall growth rate was typically 1 Å/s. All samples were grown on (001)-oriented Si substrates, which were RCA cleaned *ex situ* and underwent a thermal oxide removal at 900°C. After the deposition of a Si buffer layer, while the temperature was ramped down from approximately 600°C to the alloy growth temperature, the  $\text{Si}_{1-x-y}\text{Ge}_x\text{C}_y$  alloy layers with adjusted thicknesses have been grown. Finally, a Si cap layer has been epitaxially grown on top. The growth parameters are summarized in Table I. For background subtraction in the rBS experiments (see below), a pure Si epilayer sample was grown under the same growth conditions. Photoluminescence (PL) investigations on similar samples reveal weak  $\text{Si}_{1-x-y}\text{Ge}_x\text{C}_y$ -related features after postgrowth annealing at 650°C for 60 min. This enhancement of the PL intensity after annealing is well known from MBE-grown  $\text{Si}_{1-y}\text{C}_y$  epilayers.<sup>21</sup>

### B. X-ray diffraction

X-ray diffraction is an established method for the analysis of lattice parameters of single crystals. From the measured diffraction patterns, the lattice parameters can be extracted quite unambiguously. For many applications, e.g., for heterostructures consisting of small numbers of layers with sufficiently different lattice parameters, the latter can readily be calculated with sufficient precision from the diffraction angles via Bragg's law. For more complicated structures, algorithms based on semikinematical or dynamical scattering theory are generally used to simulate the diffraction pattern,

TABLE I. Nominal (growth) parameters of the investigated samples.

Sample	$x$ (at%)	$y$ (at%)	$d_{\text{SiGeC}}$ (nm)	$d_{\text{cap}}$ (nm)	$T_{\text{growth}}$ °C
455	10	0.40	100	100	415
453	10	0.40	100	100	415
257	10	1.00	250	50	415
454	10	1.00	100	100	415
256	10	1.00	250	50	415
573	15	0.40	50	130	425
572	15	0.75	50	130	425
460	15	1.50	100	100	415
578	15	1.15	50	130	425
459	15	1.50	100	100	415
254	15	1.30	250	50	415
462	15	1.50	100	100	415
535	20	0.40	15 :B	100 :Sb 100	425
534	20	0.40	15	200	425
536	20	0.75	15 :B	100 :Sb 100	425
532	20	0.75	15	200	425

and from a fit to the experimental data the lattice constants can be obtained. In the case of semiconductor heterostructures, however, the individual layers often do not exhibit their bulk lattice parameters, but are grown pseudomorphically or partially relaxed onto the substrate or the underlying epilayers. The resulting different strain values can be used to tailor the electrical and optical properties of such heterostructures, as many of them (e.g., band gaps and offsets, band degeneracies, etc.) depend sensitively on the lattice strain. In this case, XRD can measure the lattice plane spacings in different directions, and thus allows for the reconstruction of the distorted unit cell. For this purpose, it is necessary to measure reciprocal space maps or single scans around several reciprocal lattice points. Here, we are, however, not primarily interested in the lattice constants of a strained epilayer, but rather in the corresponding bulk lattice parameter, which we want to connect to the composition of the alloy. As it is not possible to grow the alloys under investigation as bulk materials, and not even as strain relaxed layers as in the case of binary  $\text{Si}_{1-x}\text{Ge}_x$  layers, we have to derive the data from the lattice constants of the distorted unit cells. For our  $\text{Si}_{1-x-y}\text{Ge}_x\text{C}_y$  alloys grown on (001)-oriented Si substrate and strained tetragonally, these lattice parameters are connected via the relation

$$a_{\perp}(x,y) = a_{\text{bulk}}(x,y) + 2 \frac{C_{12}(x,y)}{C_{11}(x,y)} (a_{\text{bulk}}(x,y) - a_{\parallel}), \quad (1)$$

where  $a_{\parallel}$  is the in-plane lattice constant,  $a_{\perp}$  the lattice parameter in growth direction,  $a_{\text{bulk}}(x,y)$  the bulk lattice parameter of the alloy with given Ge and C contents  $x$  and  $y$ , respectively, and  $C_{ij}(x,y)$  are its elastic constants. To determine  $a_{\text{bulk}}(x,y)$ , the elastic constants have to be known as a function of composition. It is not possible to obtain these data from our experiments, so on this point we have to rely on an assumption. The simplest one is again the linear interpolation between the values of the elements,

$C_{ij}(x,y) = (1-x-y)C_{\text{Si},ij} + xC_{\text{Ge},ij} + yC_{\text{C},ij}$ . This assumption can be made, in fact it introduces only a ‘‘second order effect’’ for the evaluation of the composition dependence of the lattice parameter, and the estimated error is below the experimental uncertainty of our study: theoretical calculations of the alloy properties performed by one of the authors<sup>7,8</sup> predict and quantify the deviations of the elastic constants from the linear interpolation. Taking into account these deviations for the calculations of the bulk lattice parameter from  $a_{\perp}(x,y)$  by means of Eq. (1), results in a small error of at most  $10^{-3}$  Å, which is approximately the precision of our XRD measurements. Based on these considerations, it is reasonable to attribute possible departures from Vegard’s rule of  $a_{\perp}(x,y)$  mainly to the volumetric rather than to elastic properties of  $\text{Si}_{1-x-y}\text{Ge}_x\text{C}_y$  alloys.

To ensure that the layers are grown pseudomorphically, we recorded reciprocal space maps around the symmetrical (004) and asymmetrical (224) Bragg reflection. Two pairs of maps have been measured in two (110) azimuths different by  $90^{\circ}$ , to ensure that the distortion of the layers is indeed tetragonal. The lattice constant in the growth direction has been obtained from fits using dynamical scattering theory to rocking curves ( $\omega$ - $2\theta$  scans) around the symmetrical (004) Bragg reflection. From these data, the bulk lattice constant of each sample has been calculated with the linearly interpolated  $C_{ij}(x,y)$ , using the absolute Ge and C concentrations of the samples, which have been obtained by applying ion backscattering techniques.

### C. Rutherford and resonant backscattering spectroscopy

The sample composition was measured by means of  $\alpha$ -particle backscattering techniques performed at the AN2000 and CN Van de Graaff accelerator facilities at the Laboratori Nazionali di Legnaro. More details about the experimental setups and analysis have been published elsewhere.<sup>22</sup>

Conventional Rutherford backscattering spectrometry (RBS), carried out with a 2 MeV  $^4\text{He}^+$  ion beam provides a determination of the Ge fraction and layer thickness. The RBS spectra were collected while rotating the sample around a [111] axial direction, with an azimuth angle of  $5^{\circ}$ . This procedure allows the smoothing of every channeling effect and provides a result (random spectrum), which is equivalent to what would be obtained from amorphous samples.<sup>23</sup> The random RBS spectra were analyzed by fitting the experimental data with numerically calculated spectra, considering geometrical factors and stopping power functions.<sup>24,25</sup>

As the simulation is obtained neglecting the C fraction, the deduced Ge concentration is affected by a systematic error which can easily be corrected after the C concentration was found. The overall typical error on the final Ge concentration measured with this procedure is about  $\pm 0.4$  at%. No information about the C content can be gained from 2 MeV spectra, mainly because of the very low value of the Rutherford cross section of this element and the low absolute C content of the samples.

An effective method to improve the ability to detect and quantify carbon atoms in silicon-based alloys is to exploit the resonances in the elastic cross section with a technique called resonant backscattering spectroscopy (rBS). In our case, we

used a 5.72 MeV  $^4\text{He}^+$  beam achieving an enhancement by a factor of 130 of the scattering cross section with respect to nonresonant conditions. This technique results in a strong improvement of the sensitivity and accuracy of the BS measurement and is fully described in Ref. 22.

Due to its low atomic number, the rBS signal from carbon is always superimposed on a high background signal from the Si substrate. The separation of the signal from C in the layer is achieved with very good accuracy by subtracting a reference spectrum collected from the pure silicon sample.

### D. Substitutional carbon fraction

In the Introduction, we have briefly addressed the problem of the lattice location of carbon. It has been shown (see, e.g., Ref. 26 and references therein) that, in spite of the extremely low bulk solubility, carbon in diluted  $\text{Si}_{1-y}\text{C}_y$  and  $\text{Si}_{1-x-y}\text{Ge}_x\text{C}_y$  alloys is mainly incorporated substitutionally. However, it is well known that carbon is also introduced to a certain amount at interstitial sites in the Si or  $\text{Si}_{1-x}\text{Ge}_x$  matrix, depending on the growth parameters, as growth temperatures and/or relative C flux.

The effect of interstitial carbon on the lattice parameter is expected to be quite different from that produced by substitutional carbon. While there exist theoretical predictions about the influence of interstitial carbon on the lattice strain,<sup>10</sup> for  $\text{Si}_{1-y}\text{C}_y$  binary alloys several experimental papers<sup>18,27-29</sup> propose virtually no effect of nonsubstitutional carbon on the lattice parameter, which we could recently confirm.<sup>15</sup> Hence, in addition to the total C concentration, the substitutional fraction has also to be measured. Furthermore, care has to be taken when comparing XRD and rBS/RBS results: while XRD is virtually ‘‘blind’’ to the interstitial fraction of C, random rBS spectra measure the *total* amount of C incorporated in the sample.

The channeling effect, used in conjunction with rBS, provides information about the site position and in particular allows us to measure the substitutional fraction of C atoms. This procedure is illustrated in Fig. 1. Panel (a) shows two rBS signals from carbon; the solid line corresponds to a random spectrum, while the dashed line refers to the corresponding signal in the channeling spectrum, collected aligning the incident beam with a (110) crystal plane,  $60^{\circ}$  off the sample normal. The decrease in the scattering yield relative to the constituent elements, quantified by the ratio  $\chi = I_{\text{aligned}}/I_{\text{random}}$  ( $I_{\text{aligned}}$  and  $I_{\text{random}}$  are the aligned and random total yields, respectively), contains information about the substitutional fraction of the species. The carbon (germanium) substitutional fraction can be determined by comparing the C (Ge) minimum yield with the matrix (Si) minimum yield:  $f = (1 - \chi_{\text{C(Ge)}})/(1 - \chi_{\text{Si}})$ . This formula gives the correct result provided the angular dips relative to Ge and C along the channeling direction have the same width.<sup>23</sup> Figure 1(b) shows an angular scan around [111] axial direction. The Si and Ge normalized yields are identical inside the error bars: this demonstrates that Ge is totally substitutional in the Si matrix. The C channeling dip has the same width but a higher value of the minimum yield  $\chi$ , indicating that, although the main C fraction is coherent with the  $\text{Si}_{1-x}\text{Ge}_x$  matrix, in the present sample, C atoms are partly located off the lattice sites.

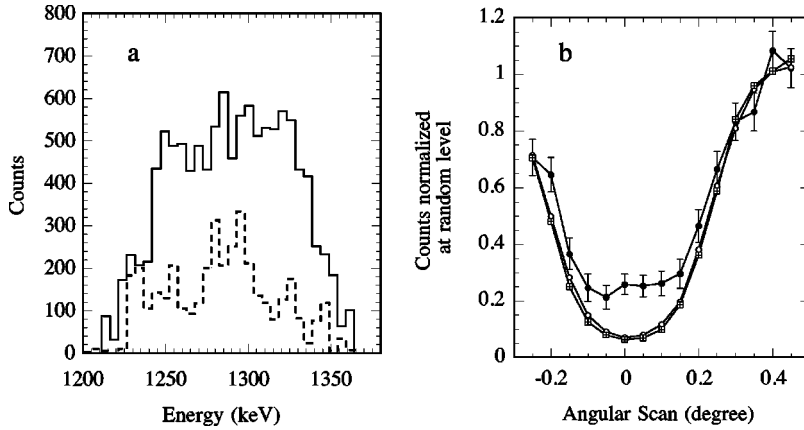


FIG. 1. rBS channeling analysis of the substitutional C fraction. In panel (a) the C signal, after the background subtraction, of a random spectrum (solid line) and an aligned spectrum (dashed line) relative to sample no. 460 is shown. In panel (b) the Si (open circles), Ge (square), and C (full circles) channeling dips across the [111] axis of sample no. 254 are shown. The yields are normalized to their random levels.

### E. SIMS measurements

The samples grown with a concentration higher than 20 at% of Ge had a layer thickness of about 15 nm, as these structures are designed for the fabrication of HBT's. With this high Ge and C contents, significantly thicker layers cannot be grown defect-free.

This thickness value is below the depth resolution of the rBS technique. Therefore, in order to determine the C and Ge concentrations of these samples we performed SIMS measurements. The samples were analyzed using a Cameca IMS-4f spectrometer with a 200 nA  $O_2^+$  beam at 1.75 keV scanned over  $250 \times 250 \mu\text{m}^2$  while sampling from a central area of  $30 \mu\text{m}$  in diameter. The depth resolution of these measurements is about 4–5 nm full width at half maximum (FWHM). The signals of the  $^{12}\text{C}^+$ ,  $^{30}\text{Si}^+$ ,  $^{76}\text{Ge}^+$  secondary ions were collected. The germanium and carbon concentrations were determined from the ratio of the  $^{76}\text{Ge}^+$  and the  $^{12}\text{C}^+$  yields, respectively, to the average value of the  $^{30}\text{Si}^+$  yield in the Si cap of the samples. This ratio was converted

to atomic concentration by measuring reference sample no. 460 (see Table II) with a composition known from a previous RBS calibration. The above procedure allows the reduction of errors due to the beam and spectrometer instabilities from measurement to measurement. The estimated relative error on the measured compositions is of about 8%. As the SIMS technique is sensitive only to the total C amount present in the epilayers, no direct information about the substitutional fraction is actually available for this series of samples.

### III. THEORETICAL METHODS

The theoretical description of  $\text{Si}_{1-x-y}\text{Ge}_x\text{C}_y$  alloys given in this work is based on Monte Carlo simulations within the empirical potential approach. The reasons for choosing this methodology and its fundamental background are explained below.

The key point in the theoretical discussion of the struc-

TABLE II. Experimental results of the investigated sample series: Ge and C concentrations  $x$  and  $y$ , substitutional C fractions  $f$  have been obtained by RBS and rBS, the lattice parameters  $a_{\text{SiGeC}}$  were obtained by XRD.

Sample	$x$ (at%)	$y$ (at%)	$f$	$yf$ (at%)	$a_{\perp}$ (Å)	$a_{\text{SiGeC}}(x,y)$ (Å)	$a_{\text{SiGe}}(x)$ (Å)	$\delta a_{\text{C}}(x,y)$ (Å)
455	10.5	$0.36 \pm 0.05$	$1.00 \pm 0.14$		5.453	5.443	5.452	$-0.009 \pm 0.001$
453	9.5	$0.56 \pm 0.09$	$1.00 \pm 0.09$		5.442	5.437	5.450	$-0.013 \pm 0.001$
257	10.0	$0.82 \pm 0.03$	$1.00 \pm 0.09$		5.430	5.430	5.451	$-0.021 \pm 0.001$
454	8.4	$0.93 \pm 0.06$	$0.99 \pm 0.05$		5.423	5.426	5.448	$-0.022 \pm 0.001$
256	9.8	$0.97 \pm 0.03$	$1.00 \pm 0.08$		5.423	5.426	5.450	$-0.024 \pm 0.001$
573	16.4	$0.31 \pm 0.06$	$1.00 \pm 0.17$		5.476	5.457	5.465	$-0.008 \pm 0.002$
572	15.2	$0.74 \pm 0.09$	$0.94 \pm 0.09$		5.449	5.441	5.462	$-0.021 \pm 0.002$
460	16.0	$1.00 \pm 0.05$	$0.91 \pm 0.05$	$0.91 \pm 0.07$	5.452	5.443	5.463	$-0.020 \pm 0.001$
578	15.1	$1.19 \pm 0.09$	$0.89 \pm 0.09$	$1.06 \pm 0.13$	5.435	5.433	5.462	$-0.029 \pm 0.002$
459	17.6	$1.28 \pm 0.06$	$0.91 \pm 0.04$	$1.16 \pm 0.07$	5.450	5.442	5.467	$-0.025 \pm 0.001$
254	15.1	$1.46 \pm 0.03$	$0.79 \pm 0.05$	$1.15 \pm 0.10$	5.430	5.430	5.462	$-0.031 \pm 0.001$
462	15.8	$1.81 \pm 0.07$	$0.77 \pm 0.03$	$1.39 \pm 0.08$	5.426	5.428	5.464	$-0.035 \pm 0.001$
535	20.4	$0.38 \pm 0.03$	<i>n.m.</i>		5.492	5.466	5.473	$-0.007 \pm 0.002$
534	22.1	$0.38 \pm 0.03$	<i>n.m.</i>		5.496	5.468	5.476	$-0.008 \pm 0.002$
536	21.8	$0.78 \pm 0.06$	<i>n.m.</i>		5.478	5.458	5.476	$-0.018 \pm 0.002$
532	25.6	$0.86 \pm 0.07$	<i>n.m.</i>		5.486	5.463	5.484	$-0.021 \pm 0.003$

tural properties of these alloys lies in the proper incorporation of carbon atoms in the lattice. Here, we focus on small carbon contents at which carbon enters substitutionally. This requires the identification of the most favorable configurations involving carbon which minimize the strain in the lattice. These geometries are metastable. In principle, under thermodynamic equilibrium, they should reorganize to form zinc-blende ( $\beta$ )-SiC (but not  $\beta$ -GeC, which is unstable; see Ref. 30) and pure  $\text{Si}_{1-x}\text{Ge}_x$ . However, this is inhibited at typical growth temperatures because bulk diffusion is very slow. It only occurs at high postgrowth annealing temperatures.<sup>31,32</sup> We thus describe them as being in “quasi-equilibrium.”

The identification of such favorable configurations must be done in the statistically proper way. Static calculations on a limited number of configurations, generated by inserting randomly carbon atoms in the lattice, can not arrive even at a minimum level of equilibration, because they are done at zero temperature, include only positional contributions to the free energy, and thus cannot capture the important aspects of the problem at finite temperatures. The proper approach is to minimize Gibb’s free energy at finite temperatures, which means to simulate atomic diffusion so that statistical-ensemble averages are taken.

We achieve this goal by utilizing Ising-type atomic flips (atom-identity switches), instead of actually simulating diffusion of atoms in the network. The latter requires the use of molecular dynamics (MD) simulations which, however, fail to reach equilibrium in practical times because of the extremely slow diffusion in the bulk. The former procedure is very powerful and for alloys with relatively small atomic size mismatch, like  $\text{Si}_{1-x}\text{Ge}_x$ , it is straightforward.<sup>33–36</sup> For systems with large size mismatch, as in the present case, the flips are energetically very costly. The difficulty is overcome by using a state-of-the-art MC algorithm,<sup>6,8</sup> that significantly enhances the phase-space sampling over the metastable configurations of the alloy.

The underlying statistical ensemble is the *semigrand* canonical (SGC) ensemble, denoted as  $(\Delta\mu, N, P, T)$ . It allows fluctuations in the number of atoms of each species (but keeping the total number of atoms  $N$  fixed) as a result of exchanges of particles within the system, driven by the appropriate chemical potential differences ( $\Delta\mu = \mu_i - \mu_j$ ,  $i, j \equiv \text{Si, Ge, C}$  in the present case). The identity flips are coupled with appropriate relaxations of nearest-neighbor ( $nn$ ) atoms, so as to lower the high barriers for diffusion in systems characterized by large atomic size mismatch and make the flips less costly. The SGC ensemble can be viewed as a special case of the grand canonical ensemble  $(\mu, V, T)$ , obtained by imposing the constraint that  $N = \sum_i N_i$  is fixed and changing to constant pressure.

The implementation of this ensemble is done through the Metropolis algorithm in the following way: The change in the potential energy of the alloy at a given MC step is a sum of three terms:

$$\begin{aligned} \Delta U(s^N) = & \Delta U_{\text{displ}}(s^N \rightarrow s'^N) + \Delta U_{\text{flip}}(s^N) \\ & + \Delta U_{\text{relax}}(s^N \rightarrow s'^N), \end{aligned} \quad (2)$$

where  $s^N$  is symbolic for the  $3N$  scaled atomic coordinates in the cell. The first term is the change due to random displace-

ments, the second is due to identity flips, and the third is due to the accompanying relaxations. The traditional random atomic moves ( $s^N \rightarrow s'^N$ ), and the volume changes  $V \rightarrow V'$  are accepted with a probability

$$P_{\text{acc}} = \min[1, \exp(-\beta\Delta W)] \sim e^{-\Delta W/k_B T}, \quad (3)$$

where

$$\Delta W = \Delta U_{\text{displ}}(s^N \rightarrow s'^N) + P(V' - V) - Nk_B T \ln(V'/V), \quad (4)$$

as in the more familiar isobaric-isothermal  $(N, P, T)$  ensemble. For the trial moves which select one of the  $N$  particles at random, and with equal probability change its identity into one of the other possible identities of the system, the acceptance probability is given by

$$\begin{aligned} P_{\text{acc}}^{\text{idn}}(i \rightarrow i') = & \min \left[ 1, \frac{\lambda_{i'}}{\lambda_i} \exp(-\beta\Delta\tilde{U}(s^N)) \right] \\ & \sim e^{\beta\Delta\mu} e^{-\beta\Delta\tilde{U}(s^N)}, \end{aligned} \quad (5)$$

where  $\lambda_i = e^{\mu_i/k_B T}$  are the fugacities in the system.  $\Delta\tilde{U}(s^N)$  denotes the change in potential energy due to the identity ( $i \rightarrow i'$ ) flip and the accompanying relaxations, so it is the combined effect of the last two terms in Eq. (2). Details about how the relaxations are performed can be found elsewhere.<sup>8</sup>

The rather complicated MC algorithm described above, with many interdependent kinds of moves, makes it prohibitively difficult at present to use energies [entering Eq. (2)] derived from *ab initio*, or even tight-binding calculations. So, the interatomic interactions in the alloy in the present work are modeled within the empirical potential approach, which lacks quantum-mechanical information but allows for much greater statistical precision and the use of large cells, compensating in part the sacrifice in accuracy. We use the potentials of Tersoff for multicomponent systems,<sup>37</sup> which have been extensively tested and applied with success in previous simulations of  $\text{Si}_{1-x-y}\text{Ge}_x\text{C}_y$  (Ref. 6),  $\text{Si}_{1-x}\text{C}_x$  (Ref. 14), and  $\text{Ge}_{1-x}\text{C}_x$  alloys (Ref. 30). Various predictions made in these works are verified experimentally.<sup>16,15,38</sup> The potentials have been shown, by comparison to accurate *ab initio* calculations,<sup>39</sup> to describe strained configurations reasonably well.

The simulations are performed using cubic supercells of 512 atoms and with periodic boundary conditions applied in all three directions. To generate the alloy formation we start with either pure Si cells or  $\text{Si}_{1-x}\text{Ge}_x$  cells of certain composition. A controlled incorporation of substitutional atoms and subsequent equilibration is achieved by choosing the appropriate chemical potential differences at typical growth temperatures. In practice, we choose a value for  $\Delta\mu_{\text{Si-Ge}}$  that we keep constant while we vary the  $\Delta\mu_{\text{Si-C}}$  to increasing values to obtain the desired carbon content. Initial values of the chemical potentials to start with are the cohesive energies per atom of the respective bulk crystal:  $\mu_{\text{C}} = -7.37$  eV,  $\mu_{\text{Si}} = -4.63$  eV,  $\mu_{\text{Ge}} = -3.85$  eV.

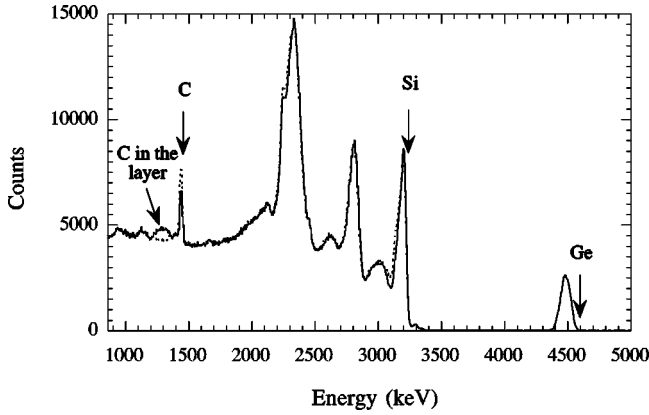


FIG. 2. rBS spectrum of sample no. 460, recorded at a primary beam energy of 5.72 MeV (solid line), and of a reference Si sample (dotted line). The signals due to Ge, Si, and C are indicated. The C signal is superimposed to a large background from Si, which is non-Rutherford in this energy range.

#### IV. RESULTS

Figure 2 shows a complete rBS spectrum of sample no. 460. The width of the well isolated Ge signal is enlarged by the superposition of signals from the Ge isotopes, which are kinematically shifted in energy. The part of the spectrum below 3260 keV is mainly due to scattering from silicon; the sequence of peaks reveals the complex energy dependence of the scattering cross section. The C signal lies below 1500 keV; to put it in better evidence, the sample spectrum is superimposed to the reference Si spectrum used for the background subtraction procedure. The role of the Si cap is to accomplish an energy separation between the rBS signals from carbon in the epilayer and the surface C contamination which is always present at the sample surface.

Figure 3 shows the (004) rocking curves of sample nos. 455 and 462, measured with XRD. The experimental data are represented by the thicker lines, whereas the thin solid lines are simulations using dynamical scattering theory. From these scans, the perpendicular lattice parameter of the samples has been determined. To ensure that the samples are fully pseudomorphic, RSM's around (004) and (224) reciprocal lattice points (RLPs) have been recorded. As an example, maps of sample no. 455 are displayed in Fig. 4.

In Table II, the Ge and C concentrations, the substitutional C fraction as well as  $a_{\perp}$  and  $a_{\text{bulk}}$ , are given for each sample. The data in the table are divided into four groups.

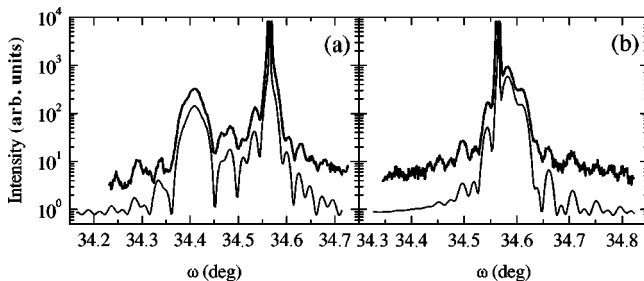


FIG. 3. XRD  $\omega$ - $2\theta$  scans around the (004) Bragg reflection of sample nos. 455 (a) and 462 (b). The thicker lines represent the experimental data, the thin solid lines are fits using dynamical scattering theory. For sample parameters see Tables I and II.

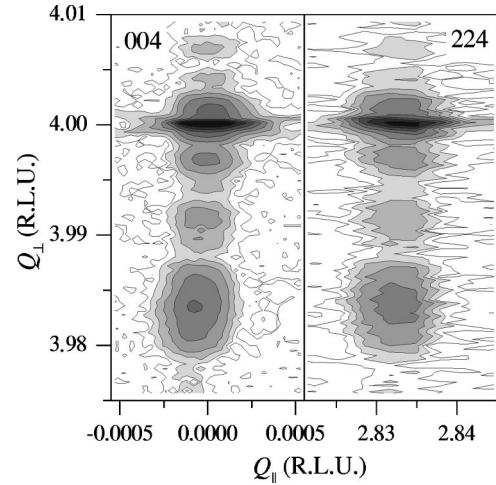


FIG. 4. XRD reciprocal space maps around the (004) and (224) reciprocal lattice points of sample no. 455. From the maps it is obvious that the  $\text{Si}_{1-x-y}\text{Ge}_x\text{C}_y$  epilayer is grown pseudomorphically with respect to the Si substrate. Isointensity contours are drawn at powers of  $10^{0.3}$  cps, starting at 0.3 cps.

The first one is relative to the series of samples with a Ge content of about 10 at%; the second group is relative to a few samples of the series with an average Ge concentration of 15 at%. The measured C concentrations of these groups of samples range from 0.3 to 1 at%, and the C substitutional fraction is unity inside the error bars. The third group is relative to the other samples of the 15 at% Ge series, where C has been found to be not fully substitutional. The fourth group is the series of samples with a Ge concentration higher than 20 at% (22 at% average) and a small (15 nm) thickness. As explained before, for this set of samples it was not possible to measure the C substitutional fraction. However, as the C total content is below 1 at%, and within this range all the other samples are fully substitutional independently of the Ge concentration, it appears reasonable to assume that the substitutional fraction of these samples is also equal to unity.

#### V. DISCUSSION

As already pointed out in the Introduction, the relaxed lattice parameters of the binary alloys  $\text{Si}_{1-x}\text{Ge}_x$  and  $\text{Si}_{1-y}\text{C}_y$  are not described by Vegard's rule (linear interpolation).<sup>11,14</sup> Indeed, it is well known that a more suitable approximation for the variation of the lattice parameter as a function of the alloy composition is given by the parabolic laws

$$a_{\text{SiGe}}(x) = (1-x)a_{\text{Si}} + xa_{\text{Ge}} + x(1-x)\theta_{\text{SiGe}}, \quad (6)$$

and

$$a_{\text{SiC}}(y) = (1-y)a_{\text{Si}} + ya_{\text{C}} + y(1-y)\theta_{\text{SiC}}, \quad (7)$$

where the deviation from linear behavior is quantified in terms of the bowing parameters  $\theta_{\text{SiGe, SiC}}$ . In order to determine and quantify with accuracy the bowing effect in the ternary alloy, we analyzed our experimental data as well as the results of Monte Carlo simulations using the following procedure. We assume that the ternary alloy is composed of a  $\text{Si}_{1-x}\text{Ge}_x$  and a  $\text{Si}_{1-y}\text{C}_y$  component. Then, in the spirit of

Eqs. (6) and (7), we may express the lattice parameter of the ternary  $\text{Si}_{1-x-y}\text{Ge}_x\text{C}_y$  alloy as an expansion up to second order in  $x$  and  $y$ :

$$a_{\text{SiGeC}}(x,y) = (1-x-y)a_{\text{Si}} + xa_{\text{Ge}} + ya_{\text{C}} + x(1-x)\theta_{\text{SiGe}} + y(1-y)\theta_{\text{SiC}} + xym. \quad (8)$$

The first three terms arise from the ‘‘conventional’’ linear interpolation (Vegard’s rule) between the diamond-phase lattice parameters of the pure elements,  $a_{\text{Si}}$ ,  $a_{\text{Ge}}$ , and  $a_{\text{C}}$ . The fourth and fifth terms take into account the lattice constant bowings in the  $\text{Si}_{1-x}\text{Ge}_x$  and  $\text{Si}_{1-y}\text{C}_y$  components, considered independently. The last term,  $xym$ , describes the bowing effect on the lattice constant arising from possible correlations between the C and Ge contents in the Si matrix, and so it couples the fourth and fifth terms.

Considering now the difference in lattice parameters between a  $\text{Si}_{1-x-y}\text{Ge}_x\text{C}_y$  alloy and the  $\text{Si}_{1-x}\text{Ge}_x$  alloy with the same Ge content  $x$ , we have

$$\begin{aligned} \delta a_{\text{C}}(x,y) &= a_{\text{SiGeC}}(x,y) - a_{\text{SiGe}}(x) \\ &= y(a_{\text{C}} - a_{\text{Si}}) + y(1-y)\theta_{\text{SiC}} + xym. \end{aligned} \quad (9)$$

This equation is the benchmark to which both the experimental and theoretical results are referred. We first present the analysis of the experimental data. The lattice constant  $a_{\text{SiGeC}}(x,y)$  can be derived from XRD measurements inverting Eq. (1), and  $a_{\text{SiGe}}(x)$  can be calculated from the RBS value for  $x$  using Eq. (6). The lattice parameter values of the constituent elements used for the derivations are  $a_{\text{Si}} = 5.43102 \text{ \AA}$ ,  $a_{\text{Ge}} = 5.6579 \text{ \AA}$ ,  $a_{\text{C}} = 3.5668 \text{ \AA}$  (see Ref. 40);  $\theta_{\text{SiGe}} = -0.026 \text{ \AA}$  is derived from the data in Ref. 11. The values for  $a_{\text{SiGeC}}(x,y)$ ,  $a_{\text{SiGe}}(x)$ , and  $\delta a_{\text{C}}(x,y)$  derived from our experimental data are reported in Table II.

The term  $y^2\theta_{\text{SiC}}$  in Eq. (9) is at most  $2 \times 10^{-4} \text{ \AA}$  in our range of C concentrations, which is significantly smaller than the XRD precision, and is hence neglected. Doing this,  $\delta a_{\text{C}}(x,y)$  depends linearly on  $x$  and  $y$ :

$$\delta a_{\text{C}}(x,y) = y(a_{\text{C}} - a_{\text{Si}} + \theta_{\text{SiC}} + xm), \quad (10)$$

i.e., the deformation induced by the introduction of *small amounts* of C in the  $\text{Si}_{1-x}\text{Ge}_x$  matrix is expected to be directly proportional to the C concentration, with a proportionality constant  $(a_{\text{C}} - a_{\text{Si}} + \theta_{\text{SiC}} + xm)$ . The term  $a_{\text{C}} - a_{\text{Si}}$  would be the only term in the case of validity of Vegard’s rule;  $\theta_{\text{SiC}}$  accounts for the deviation from Vegard’s rule due to the  $\text{Si}_{1-y}\text{C}_y$  component, and  $xm$  takes into account the possible influence of the Ge concentration on the capability of C to change the matrix ( $\text{Si}_{1-x}\text{Ge}_x$ ) volume.

The experimental values of  $\delta a_{\text{C}}$  are plotted as a function of the C concentration in Fig. 5. Different symbols denote the individual series with different Ge content. We included also the data set for the pure  $\text{Si}_{1-y}\text{C}_y$  samples of Ref. 15. For the 15 at% Ge series (triangles) full symbols refer to the total C concentration, while open symbols refer to the substitutional C concentration. In the case of  $\text{Si}_{1-y}\text{C}_y$  the lattice contraction due to the incorporation of substitutional carbon should still be described by Eq. (10) which reduces to  $(a_{\text{C}} - a_{\text{Si}} + \theta_{\text{SiC}})$  ( $x=0$ ). The solid lines represent the theoretical results (see below).

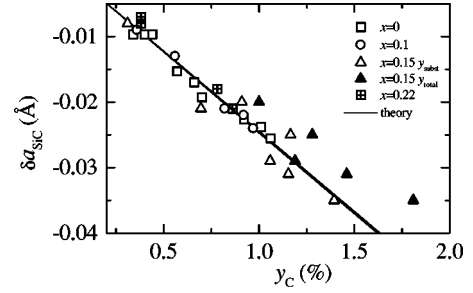


FIG. 5. Difference in bulk lattice parameters  $\delta a_{\text{C}} = a_{\text{SiGeC}} - a_{\text{SiGe}}$  for the investigated sample series. Open symbols are referred to the substitutional C concentration ( $fy$ ). The full triangles are plotted against the total C amount. The window symbol corresponds to thin  $\text{Si}_{1-x-y}\text{Ge}_x\text{C}_y$  epilayers, where no substitutional fraction could be determined experimentally.

Up to a C content of 1 at%, all the series strongly correlate with the linear behavior, independent of the Ge concentration. Only the 15% series (full triangles in Fig. 5) does not coincide with the other data. This is, however, only true as long as the *total* C content as derived from rBS is used in our analysis. If we only consider the amount of C in *substitutional* lattice sites (open triangles), then these data can as well be described by Eq. (10). This strongly indicates that only the substitutional C fraction contributes to the average strain in  $\text{Si}_{1-x-y}\text{Ge}_x\text{C}_y$  epilayers (i.e., XRD is virtually ‘‘blind’’ for nonsubstitutional carbon). The samples with 22 at% Ge concentration (window symbol in Fig. 5) agree very well with the general behavior of the fully substitutional samples, indirectly suggesting that carbon is fully substitutional in these samples (otherwise the data would be shifted to smaller  $y$ ). In Ref. 10, Windl *et al.* theoretically predicted the lattice strain caused by interstitial carbon. They find two inequivalent lattice sites,  $\text{C}_{\parallel}$  and  $\text{C}_{\perp}$ . While C in the first site doesn’t give rise to lattice strain, C in the second site significantly *expands* the lattice. We have no direct information on the occupation of the two interstitial sites from our experimental data, however, we can only *consistently* interpret our data if we assume that interstitial carbon produces virtually no strain.

The parameters  $\theta_{\text{SiC}}$  and  $m$  have been obtained from a linear fit to  $\delta a_{\text{C}}/y$  as a function of the Ge content  $x$  [see Eq. (10)]:

$$\theta_{\text{SiC}} = -0.64 \pm 0.09 \text{ \AA},$$

$$m = 0.5 \pm 0.7 \text{ \AA}.$$

The parameter  $m$  is hence very close to zero within the experimental error, indicating that the dependence of the lattice contraction, caused by C, on the Ge content is weak [note that in Eq. (9) the influence on the lattice parameter is  $mxy$ , i.e.,  $m$  is multiplied with two small numbers]. We discuss the magnitude of  $\theta_{\text{SiC}}$  below.

The theoretical data presented in this work are the result of direct MC simulations of the equilibrium structure and composition of the ternary alloy. The simulations are based on the methodology described in Sec. III. The central quantity of interest is the relaxed lattice constant  $a_0(x,y)$ . We also calculate the corresponding lattice constant  $a_0(x)$  of the

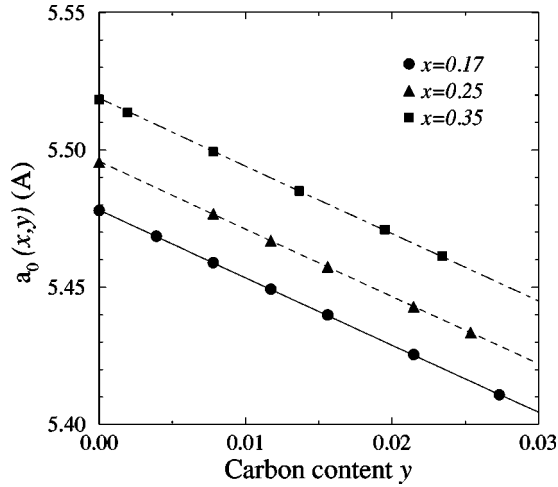


FIG. 6. Theoretical lattice parameters plotted against the carbon content  $y$ . Different symbols indicate different Ge compositions.

binary  $\text{Si}_{1-x}\text{Ge}_x$  alloy. We wish to present the values of  $a_0(x,y)$  at room temperature. Since atom-identity flips for the generation of cells are rare at such low temperatures, we use the following procedure. Three different configurations for each  $x,y$  at 900 K (typical growth temperature) are generated using the SGC ensemble. Then we switch to the  $N,P,T$  ensemble, so eliminating the chemical-potential dependence and fixing the composition, in order to average over the cell dimensions for thousands of MC steps at 300 K to obtain  $a_0$  for each configuration. Averaging over the three configurations gives  $a_0$  for each  $x,y$ .

The results of these extensive calculations for the lattice constants as a function of carbon content  $y$  for three different Ge concentrations  $x$  are shown in Fig. 6, the corresponding  $\delta a_C$  values are plotted as solid lines in Fig. 5. In order to have a direct and consistent comparison with our experimental data, we limit the carbon contents to  $\sim 3$  at%. From a linear fit to the  $\delta a_C/y$  values derived from the theoretical data we obtain

$$\theta_{\text{SiC}} = -0.59 \pm 0.005 \text{ \AA}$$

$$m = 0.06 \pm 0.02 \text{ \AA}.$$

Thus, our theoretical analysis confirms and strengthens the conclusion derived from the experimental data about the bowing effect in the ternary alloy: this is nearly independent of the correlation between the Ge and C contents  $x,y$ , since the parameter  $m$  is negligibly small. The explanation of this behavior is easily understood by recalling that there is a remarkable interaction between Ge and C atoms in the Si lattice. As shown previously,<sup>6,8</sup> there is a strong repulsive Ge–C interaction which prevents the two species from approaching at first–nearest-neighbor positions, while forces the C atoms to bond solely to Si atoms, not excluding the appearance of Ge–Si–C bonds (second neighbors). These tendencies hold for *any appreciable* Ge composition, at which the incorporated C atoms have a significant probability to interact with Ge atoms. This is true for the Ge contents studied here, and since the microscopic environment of C atoms is similar in these cases, the bowing effect is insensitive to the Ge content.

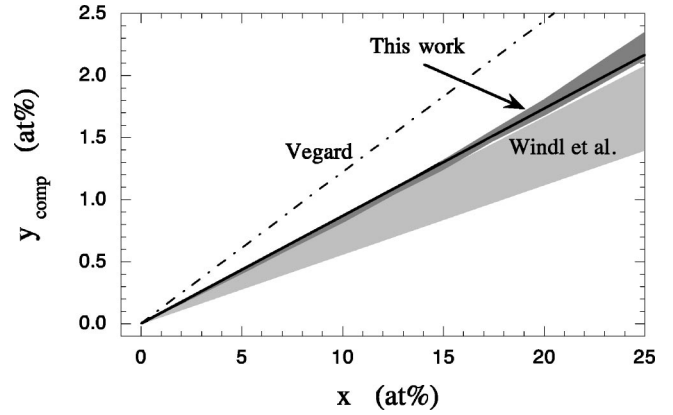


FIG. 7. Plot of the C concentration needed in order to compensate the compressive strain induced by Ge as a function of the Ge concentration. The theoretical results coming from this work are represented as a solid line. This line lies inside a dark area which is calculated using the values of  $m$  and  $\theta_{\text{SiC}}$  following our experimental data. The area width takes the experimental error bars into account. For comparison, the compensating C concentration according to Vegard's rule (dot dashed line) and to Windl's calculations [see Ref. 10:  $y_{\text{comp}} = 1/(15 \pm 3)x$ , light area] are shown.

Regarding the bowing parameter, we see that the theoretical value of  $\theta_{\text{SiC}} = -0.59 \text{ \AA}$  is in excellent agreement with the respective theoretical value of  $-0.57 \text{ \AA}$  calculated before<sup>14</sup> with the same methodology for  $\text{Si}_{1-y}\text{C}_y$  alloys (the small difference might be attributed to the fact that the latter calculations of the lattice constants were carried out at 0 K). This shows consistency, as it is derived from two independent calculations, and it also justifies the breakup of the bowing effect in the ternary alloy into  $\text{Si}_{1-x}\text{Ge}_x$  and  $\text{Si}_{1-y}\text{C}_y$  contributions. Furthermore, the experimentally derived value of  $\theta_{\text{SiC}} = -0.64 \pm 0.09 \text{ \AA}$  and the theoretical value are in fairly good agreement, with the latter lying within experimental error. For comparison, Windl *et al.*<sup>10</sup> arrived at a much larger value ( $-1.25 \text{ \AA}$ ) for the bowing parameter in  $\text{Si}_{1-y}\text{C}_y$  alloys with a C composition lower than 3.1 at%. Only when they consider the whole composition range,  $\theta_{\text{SiC}}$  reaches a value ( $-0.69 \text{ \AA}$ ) closer to our experimental and theoretical values.

Having settled the issue of the bowing effect, we are now in a position to calculate the exact amount of carbon needed to compensate the tensile strain introduced by germanium. From Eq. (8) and by putting  $a_{\text{SiGeC}}(x,y)$  equal to  $a_{\text{Si}}$ , one obtains

$$y = -x(a_{\text{Ge}} - a_{\text{Si}} + (1-x)\theta_{\text{SiGe}})(a_{\text{C}} - a_{\text{Si}} + \theta_{\text{SiC}} + mx), \quad (11)$$

where we have neglected the term  $y^2\theta_{\text{SiC}}$  as previously done. The compensating ratio  $x/y$  can be directly derived from Fig. 7, where we have summarized our experimental and theoretical results. The theoretical values are given by the solid line which lies within the darker area representing the experimental determination of  $m$  and  $\theta_{\text{SiC}}$ . Its width increases with Ge concentration because the errors in evaluating  $m$  and  $\theta_{\text{SiC}}$  have been taken into account. As a comparison, the corresponding calculated values assuming the validity of Vegard's rule (broken line) and by considering the results of Ref. 10 are reported (lighter area). The compensating ratio derived

from Fig. 7 is  $\nu=12$ , significantly higher than the value  $\nu=8.2$  expected from Vegard's rule, and at the limit of the error bar from the value found by Windl *et al.*,  $\nu=15\pm 3$ .

## VI. SUMMARY

We have investigated several series of  $\text{Si}_{1-x-y}\text{Ge}_x\text{C}_y$  samples with different Ge and C concentrations up to 0.25 and 0.02, respectively. We have determined the lattice parameter of the ternary alloys by XRD diffraction, whereas the  $x$  and  $y$  compositions were determined by RBS and rBS techniques. The substitutional fraction of carbon atoms was measured by means of channeling techniques. Detailed MC simulations were carried out to compute the structural parameters of the alloys. The measured values of  $a_{\text{SiGeC}}(x,y)$  are in good agreement with the theoretical predictions. A

strong deviation from Vegard's rule is found, characterized by a strain compensating ratio between Ge and C of  $\nu=12$ . Our results indicate that only the fraction of carbon substitutionally incorporated into the  $\text{Si}_{1-x}\text{Ge}_x$  matrix contributes considerably to a change of the lattice parameter, and that interstitial carbon plays a negligible role. However, further research, both experimental and theoretical, is needed to establish this result. Finally, we find that the bowing effect in the ternary alloy is nearly independent of the Ge and C contents. This can be attributed to the strong atomic Ge-C interactions that favor the same specific arrangements of species, independent of the Ge composition.

## ACKNOWLEDGMENT

This work was supported by FWF, Vienna.

- 
- \*Present address: Optoelectronics Research Centre, University of Southampton, Southampton SO17 1BJ, Great Britain.
- <sup>†</sup>Present address: TASC-INFM at Elettra Synchrotron, S.S. 14 km 163.53 4012 Basovizza-Trieste, Italy.
- <sup>1</sup>K. Eberl, K. Brunner, and O.G. Schmidt, in *Germanium Silicon, Physics and Materials*, edited by R. Hull and J.C. Bean, Vol. 56 of *Semiconductors and Semimetals* (Academic, San Diego, 1999).
- <sup>2</sup>S.C. Jain, *Germanium-Silicon Strained Layers and Heterostructures* (Academic, Boston, 1994).
- <sup>3</sup>R.A. Soref, *J. Appl. Phys.* **70**, 2470 (1991).
- <sup>4</sup>A.A. Demkov and O.F. Sankey, *Phys. Rev. B* **48**, 2207 (1993).
- <sup>5</sup>O.G. Schmidt and K. Eberl, *Phys. Rev. Lett.* **80**, 3396 (1998).
- <sup>6</sup>P.C. Kelires, *Phys. Rev. Lett.* **75**, 1114 (1995).
- <sup>7</sup>P.C. Kelires, *Appl. Surf. Sci.* **102**, 12 (1996).
- <sup>8</sup>P.C. Kelires, *Int. J. Mod. Phys. C* **9**, 357 (1998).
- <sup>9</sup>G. Theodorou, G. Tsegas, P.C. Kelires, and E. Kaxiras, *Phys. Rev. B* **60**, 11 494 (1999).
- <sup>10</sup>W. Windl, O.F. Sankey, and J. Menéndez, *Phys. Rev. B* **57**, 2431 (1998).
- <sup>11</sup>J.P. Dismukes, L. Ekstrom, and R.J. Paff, *J. Phys. Chem.* **68**, 3021 (1964).
- <sup>12</sup>S. de Gironcoli, P. Giannozzi, and S. Baroni, *Phys. Rev. Lett.* **66**, 2116 (1991).
- <sup>13</sup>G. Theodorou, P.C. Kelires, and C. Tserbak, *Phys. Rev. B* **50**, 18 355 (1994).
- <sup>14</sup>P.C. Kelires, *Phys. Rev. B* **55**, 8784 (1997).
- <sup>15</sup>M. Berti, D. De Salvador, A.V. Drigo, F. Romanato, J. Stangl, S. Zerlauth, F. Schäffler, and G. Bauer, *Appl. Phys. Lett.* **72**, 1602 (1998).
- <sup>16</sup>M. Meléndez-Lira, J. Menéndez, W. Windl, O.F. Sankey, G.S. Spencer, S. Segó, R.B. Culbertson, A.E. Bair, and T.L. Alford, *Phys. Rev. B* **54**, 12 866 (1996).
- <sup>17</sup>S. Segó, R.J. Culbertson, A.E. Bair, and T. Alford, *J. Vac. Sci. Technol. A* **14**, 441 (1996).
- <sup>18</sup>S. Zerlauth, H. Seyringer, C. Penn, and F. Schäffler, *Appl. Phys. Lett.* **71**, 3826 (1997).
- <sup>19</sup>M. Meléndez-Lira, J. Menéndez, K.M. Kramer, M.O. Thompson, N. Cave, R. Liu, J.W. Christiansen, N.D. Theodore, and J.J. Candelaria, *J. Appl. Phys.* **82**, 4246 (1997).
- <sup>20</sup>H.J. Osten, J. Griesche, and S. Scalese, *Appl. Phys. Lett.* **74**, 836 (1999).
- <sup>21</sup>C. Penn, S. Zerlauth, J. Stangl, G. Bauer, G. Brunthaler, and F. Schäffler, *J. Vac. Sci. Technol. B* **16**, 1713 (1998).
- <sup>22</sup>M. Berti, D. De Salvador, A.V. Drigo, F. Romanato, A. Sambo, S. Zerlauth, J. Stangl, F. Schäffler, and G. Bauer, *Nucl. Instrum. Methods Phys. Res. B* **143**, 357 (1998).
- <sup>23</sup>*Handbook of Modern Ion Beam Materials Analysis*, edited by J.R. Tesmer and M. Nastasi (Materials Research Society, Pittsburgh, 1995).
- <sup>24</sup>J.F. Ziegler, *Stopping Power and Ranges of Ions in Matter* (Pergamon Press, New York, 1997), Vol 4.
- <sup>25</sup>D.C. Santry and R.D. Weiner, *Nucl. Instrum. Methods* **178**, 523 (1978).
- <sup>26</sup>S.C. Jain, H.J. Osten, B. Dietrich, and H. Rücker, *Semicond. Sci. Technol.* **10**, 1289 (1995).
- <sup>27</sup>H.J. Osten, D. Endisch, E. Bugiel, B. Dietrich, G.G. Fischer, M. Kim, D. Krüger, and P. Zaumseil, *Semicond. Sci. Technol.* **11**, 1678 (1996).
- <sup>28</sup>P. Zaumseil, G.G. Fischer, K. Brunner, and K. Eberl, *J. Appl. Phys.* **81**, 6134 (1997).
- <sup>29</sup>M.S. Goorsky, S.S. Iyer, K. Eberl, F.K. LeGoues, J. Angilello, and F. Cardone, *Appl. Phys. Lett.* **60**, 2758 (1992).
- <sup>30</sup>P.C. Kelires, *Phys. Rev. B* **60**, 10 837 (1999).
- <sup>31</sup>G.G. Fischer, P. Zaumseil, E. Bugiel, and H.J. Osten, *J. Appl. Phys.* **77**, 1934 (1995).
- <sup>32</sup>P. Warren, J. Mi, F. Overney, and M. Dutoit, *J. Cryst. Growth* **157**, 414 (1995).
- <sup>33</sup>S.M. Foiles, *Phys. Rev. B* **32**, 7685 (1985).
- <sup>34</sup>P.C. Kelires and J. Tersoff, *Phys. Rev. Lett.* **63**, 1164 (1989).
- <sup>35</sup>B. Dünweg and D.P. Landau, *Phys. Rev. B* **48**, 14 182 (1993); M. Laradji, D.P. Landau, and B. Dünweg, *ibid.* **51**, 4894 (1995).
- <sup>36</sup>A. Silverman, A. Zunger, R. Kalish, and J. Adler, *J. Phys.: Condens. Matter* **7**, 1167 (1995).
- <sup>37</sup>J. Tersoff, *Phys. Rev. B* **39**, 5566 (1989).
- <sup>38</sup>H. Jacobson, J. Xiang, N. Herbots, S. Whaley, P. Ye, and S. Hearne, *J. Appl. Phys.* **81**, 3081 (1997).
- <sup>39</sup>P.C. Kelires and E. Kaxiras, *Phys. Rev. Lett.* **78**, 3479 (1997).
- <sup>40</sup>*Semiconductors-Basic Data*, edited by O. Madelung (Springer, Berlin, 1996).